# Targeted α-Therapy of Metastatic Castration-Resistant Prostate Cancer with $^{225}$Ac-PSMA-617: Dosimetry Estimate and Empiric Dose Finding

Clemens Kratochwil[1], Frank Bruchertseifer[2], Hendrik Rathke[1], Marcus Bronzel[3], Christos Apostolidis[2], Wilko Weichert[4], Uwe Haberkorn[1,5], Frederik L. Giesel[1], and Alfred Morgenstern[2]

*[1]Department of Nuclear Medicine, University Hospital Heidelberg, Heidelberg, Germany; [2]Directorate for Nuclear Safety and Security, European Commission, Joint Research Centre, Karlsruhe, Germany; [3]ABX-CRO, Dresden, Germany; [4]Institute of Pathology, University Hospital at Technical University Munich, Munich, Germany; and [5]Cooperation Unit Nuclear Medicine, German Cancer Research Center (DKFZ), Heidelberg, Germany*

The aim of this study was to develop a treatment protocol for $^{225}$Ac-PSMA-617 α-radiation therapy in advanced-stage, metastatic castration-resistant prostate cancer patients with prostate-specific membrane antigen (PSMA)–positive tumor phenotype. **Methods:** A dosimetry estimate was calculated on the basis of time–activity curves derived from serially obtained $^{177}$Lu-PSMA-617 scans extrapolated to the physical half-life of $^{225}$Ac, assuming instant decay of unstable daughter nuclides. Salvage therapies empirically conducted with 50 ($n$ = 4), 100 ($n$ = 4), 150 ($n$ = 2), and 200 kBq/kg ($n$ = 4) of $^{225}$Ac-PSMA-617 were evaluated retrospectively regarding toxicity and treatment response. Eight of 14 patients received further cycles in either 2- or 4-mo intervals with identical or deescalated activities. **Results:** Dosimetry estimates for 1 MBq of $^{225}$Ac-PSMA-617 assuming a relative biologic effectiveness of 5 revealed mean doses of 2.3 Sv for salivary glands, 0.7 Sv for kidneys, and 0.05 Sv for red marrow that are composed of 99.4% α, 0.5% β, and 0.1% photon radiation, respectively. In clinical application, severe xerostomia became the dose-limiting toxicity if treatment activity exceeded 100 kBq/kg per cycle. At 100 kBq/kg, the duration of prostate-specific antigen decline was less than 4 mo, but if therapy was repeated every 2 mo patients experienced additive antitumor effects. Treatment activities of 50 kBq/kg were without toxicity but induced insufficient antitumor response in these high-tumor-burden patients. Remarkable antitumor activity by means of objective radiologic response or tumor marker decline was observed in 9 of 11 evaluable patients. **Conclusion:** For advanced-stage patients, a treatment activity of 100 kBq/kg of $^{225}$Ac-PSMA-617 per cycle repeated every 8 wk presents a reasonable trade-off between toxicity and biochemical response.

**Key Words:** PSMA; $^{225}$Ac; targeting; prostate cancer

**J Nucl Med 2017; 58:1624–1631**
DOI: 10.2967/jnumed.117.191395

Prostate-specific membrane antigen (PSMA) targeting with $^{177}$Lu-labeled PSMA ligands presents a promising new option for salvage therapy of patients with metastatic castration-resistant prostate cancer (mCRPC) (*1–3*).

However, only 45% of patients biochemically respond (prostate-specific antigen [PSA] decline > 50%) to PSMA ligands labeled with β-emitting $^{177}$Lu, and 40% of patients do not respond at all (*2*). Targeted α-therapy (TAT) has been shown to be able to overcome resistance to β-emitters in clinical application (*4*). After binding at the tumor cell surface, PSMA ligands are internalized (*5*), which is considered particularly beneficial for short-range Auger (*6*) and α-particle radiation (*7*) and is especially important for radionuclides that decay into unstable daughter nuclides. The shorter tissue range of α-radiation also offers the potential of targeting tumor cells infiltrating bone marrow with reduced toxicity compared with β-emitters. In comparison to β-emitting bone seekers such as $^{89}SrCl_2$, the α-emitting $^{223}RaCl_2$ demonstrated improved survival of mCRPC patients while simultaneously reducing hematologic toxicity (*8*). Remarkably low hematologic toxicity has also been observed during TAT of a patient with diffuse bone metastases of neuroendocrine differentiated prostate cancer treated with $^{213}$Bi-DOTATOC (*4*). Dosimetry studies demonstrated that the salivary glands and kidneys might be dose-limiting organs for $^{177}$Lu-PSMA-617 (*1,9–11*). This is in accordance with histologic immunostainings, reporting weak physiologic PSMA expression in these tissues (*12*). If salivary gland uptake would be predominantly PSMA-specific, the microdosimetry of short range α-radiation offers promise to spare wide parts of the surrounding salivary gland tissue. Thus, based on theoretic considerations, PSMA TAT with $^{225}$Ac-PSMA-617 offers the promise to enhance treatment efficacy and simultaneously reduce toxicity. Therefore, PSMA TAT was introduced to our clinic as a salvage therapy for patients with advanced mCRPC who had exhausted approved therapies. Here we retrospectively report our clinical experience with the first patients receiving PSMA TAT with different dosing regimens of $^{225}$Ac-PSMA-617 and share the rationale of our derived treatment protocol.

## MATERIALS AND METHODS

### Patients

$^{225}$Ac-PSMA-617 was offered as salvage therapy in accordance with the updated Declaration of Helsinki, paragraph-37 "Unproven Interventions in Clinical Practice," and in accordance with German regulations for medical indication of an unapproved drug in patients who exhausted approved treatments, in particular with regard to German

Received Feb. 13, 2017; revision accepted Apr. 3, 2017.
For correspondence or reprints contact: Clemens Kratochwil, University Hospital Heidelberg, Department of Nuclear Medicine, INF 400, 69120 Heidelberg, Germany.
E-mail: clemens.kratochwil@med.uni-heidelberg.de
Published online Apr. 13, 2017.
COPYRIGHT © 2017 by the Society of Nuclear Medicine and Molecular Imaging.



UH & EURATOM Exhibit 2044-001
Fusion v. Universität Heidelberg, et al.
IPR2023-00551

pharmaceutical act §13(2b). All patients had a PSMA-positive tumor phenotype as demonstrated in a preceding PSMA PET/CT scan with $^{68}$Ga-PSMA-11 or PSMA SPECT/CT scan with $^{99m}$Tc-MIP1427. Patients were informed about the experimental nature of this therapy and gave written informed consent. Detailed patient characteristics are summarized in (Table 1). The ethical committee approved the retrospective evaluation as an observational study.

### Dosimetry Estimate

A low probability for γ-coemission and overlapping Bremsstrahlung due to β-emitters in the $^{225}$Ac decay chain (Supplemental Fig. 1; supplemental materials are available at http://jnm.snmjournals.org) preclude treatment concomitant dosimetry. Therefore, organ-absorbed doses for $^{225}$Ac-PSMA-617 were approximated by extrapolating preexisting $^{177}$Lu-PSMA-617 data. Methods for $^{177}$Lu-PSMA-617 dosimetry were already described in the supplement of a previous publication (*1*). A strength of this protocol was the inclusion of a late imaging time point 5–10 d after administration. Meanwhile these results were confirmed by other groups (*9–11*) and can be considered representative. The counts within the regions of interest of whole body and delineable organs from all imaging time points as well as activities measured in blood samples were extrapolated from the 6.7-d half-life of $^{177}$Lu to the half-life of 9.9 d of $^{225}$Ac. Time–activity curves and related area under the curve were then fitted, integrated, and normalized to residence times as already described (*13*). The kidneys, liver, spleen, bladder, red marrow, and whole-body remainder were used as source organs in OLINDA (*13*), using the adult male model with organ masses of the original phantom. The residency times of $^{225}$Ac were then forwarded as residency times of $^{221}$Fr, $^{217}$At, $^{213}$Bi, $^{213}$Po, $^{209}$Tl, and $^{209}$Pb for OLINDA calculations, assuming instant decay of the daughter nuclides without translocation during the delay between succeeding disintegrations. The relative biologic efficacy (RBE) for the α-particles emitted from $^{225}$Ac, compared with β-radiation, was assumed to be 5 according to literature (*14*). Finally, the absorbed dose of all decay steps was summed up, with weighting factors of 2% for $^{209}$Tl and 98% for $^{213}$Po to account for the 2 possible pathways in the $^{225}$Ac decay chain (Supplemental Fig. 1). The spheric model of OLINDA was used to calculate the doses for the salivary glands for individual gland volumes derived from baseline PET/CT images.

### PSMA Immunhistochemistry

PSMA immunohistochemistry was performed with a series of tissue bank samples from salivary glands, kidneys, and prostate cancer using a standard protocol analogous to the detailed description in a previous publication (*15*).

### Radiopharmaceuticals

The precursors for PSMA-11 and PSMA-617 were obtained from ABX. The precursor for MIP1427 (*16*) was synthesized in-house, $^{225}$Ac was produced by radiochemical extraction from $^{229}$Th (*17,18*), and $^{68}$Ga and $^{99m}$Tc were eluted from commercial generator systems on-site. The labeling conditions and imaging protocols for $^{68}$Ga-PSMA-11 (*19*), $^{99m}$Tc- MIP1427 (*1*), and posttherapeutic $^{225}$Ac-PSMA-617 emission scans (*20*) have been described previously.

### Determination of Treatment Activity

Because the reported patients were not treated according to a prospectively defined protocol inside a clinical trial but under the paragraph "unproven intervention in clinical practice," the treatment activity was not escalated in a systematic manner but was tailored individually by the physicians in charge, taking into account the estimated spontaneous prognosis (site of metastasis, progression velocity) and baseline laboratory tests of the respective patient. The individually

**TABLE 1**
Patient Characteristics

| Patient no. | Age (y) | Dose (kBq/kg) | Baseline PSA | Metastasis* | GnRH-A/A | Antiandrogen | Abiraterone | Enzalutamide | Docetaxel | Other systemic therapies |
|---|---|---|---|---|---|---|---|---|---|---|
| 1 | 73 | 50 | 224 | OSS, BRA | x | x | x | x | x | Ketokonazol, vinorelbine, β-PSMA ($^{131}$I) |
| 2 | 71 | 50 | 63 | LYM, OSS, HEP | x | x | | x | x | Cabazitaxel, estramustine |
| 3 | 67 | 50 | <0.1 | OSS | x | x | x | | | |
| 4 | 60 | 50 | 118 | LYM, OSS | x | x | | x | x | Cabazitaxel, $^{223}$Ra |
| 5 | 70 | 100 | 276 | LYM, OSS, PUL | x | x | x | x | x | Curevac, thalidomid, celecoxib, DOTATOC |
| 6 | 53 | 100 | 245 | LYM, OSS | x | | | | | |
| 7 | 58 | 100 | 64.7 | LYM, OSS, PUL | x | x | x | x | x | β-PSMA ($^{131}$I) |
| 8 | 78 | 100 | 420 | LYM, OSS | x | x | x | x | x | Cabozantinib |
| 9 | 79 | 150 | 1,153 | LYM, OSS | x | x | x | x | | Estramustine |
| 10 | 57 | 150 | 744 | OSS, HEP, BRA | x | x | | | x | $^{223}$Ra, β-PSMA ($^{177}$Lu) |
| 11 | 68 | 200 | <0.1 | LYM, OSS, PUL, HEP, BRA | x | x | x | | x | |
| 12 | 60 | 200 | 1,100 | LYM, OSS, HEP | x | x | x | | x | Sorafenib, TACE (Irinotecan) |
| 13 | 78 | 200 | 2,841 | LYM, OSS, HEP | x | x | x | x | x | Tasquinimod |
| 14 | 63 | 200 | 2.8 | LYM, OSS, HEP | x | x | x | x | | |

*Site of disease according to TNM classification.

GnRH-A/A = previous treatment with gonadotropin-releasing hormone analogs or antagonists; OSS = osseous; BRA = brain; LYM = lymphatic; HEP = hepatic; PUL = lung; TACE = transarterial chemoembolization.



UH & EURATOM Exhibit 2044-002
Fusion v. Universität Heidelberg, et al.
IPR2023-00551

administered activities and prognostic profiles for tailoring the patients into their particular escalation level are summarized in Table 1. According to German radiation protection regulations the patients were hospitalized as in-patients until 48 h after injection. Clinical examination was done before and 1 d after therapy. Patients received intravenous hydration (2,000 mL of 0.9% NaCl; flow, 333 mL/h) starting 30 min before therapy. The therapy solution was administered with a slow (30–60 s) freehand injection through a 0.20-μm sterile filter with low protein binding (Filtropur S 0.2). Androgen-deprivation therapy was maintained during PSMA TAT; other treatments were discontinued.

### Follow-up

Blood cell count, creatinine, blood-urea-nitrogen, liver enzymes, PSA, clinical examination, and patient anamnesis were done every 4 wk and classified into toxicity grades using the Common Terminology Criteria for Adverse Events (*21*). Imaging follow-up was performed with the identical modality (PSMA PET/CT or PSMA SPECT/CT) as

**TABLE 2**
Observed Toxicities and Further Proceedings

| Patient no. | $^{225}$Ac activity, first cycle | PLT | WBC | Hb | Xerostomia | Other | Follow-up and further proceedings |
|---|---|---|---|---|---|---|---|
| 1 | 3.3 | G4 → G4 | G2 | TD → TD | 0 | 0 | BSC; PFS 6 wk; OS 16 wk |
| 2 | 4.5 | G4 → G4 | 0 | TD → TD | 0 | 0 | OS 7 wk |
| 3 | 5 | 0 | 0 | 0 | 0 | 0 | Second cycle, 50 kBq/kg (2-mo interval) |
| | | | | | | | Third cycle, 50 kBq/kg (2-mo interval) |
| | | | | | | | Radiologic progression of disease; OS > 8 mo |
| 4 | 6 | 0 | 0 | G1 → G1 | 0 | 0 | OS 8 wk |
| 5 | 9.0 | G1 | G2 → G3 | G2 → G3 | 0 | 0 | Second cycle, 100 kBq/kg (4-mo interval) |
| | | | | | | | Third cycle, 100 kBq/kg (2-mo interval) |
| | | | | | | | Hematologic toxicity with overlap to DOTATOC followed by cabazitaxel; OS > 24 mo |
| 6 | 9.0 | NA | NA | NA | NA | NA | Combination with docetaxel 75 mg/m$^2$ → G5 neutropenia, OS 1 mo |
| 7 | 10.9 | 0 | 0 | 0 | G1 | 0 | Second cycle, 100 kBq/kg (4-mo interval) |
| | | | | | | | Third cycle, 100 kBq/kg (2-mo interval) |
| | | | | | | | OS 10 mo |
| 8 | 16.0 | 0 | 0 | 0 | G1 | 0 | Second cycle, 100 kBq/kg (2-mo interval) |
| | | | | | | | PFS 9 mo |
| | | | | | | | Third cycle, 100 kBq/kg (start of second series) |
| | | | | | | | Fourth cycle, 100 kBq/kg (2-mo interval) |
| | | | | | | | OS 17 mo |
| 9 | 13.4 | 0 | 0 | G2 → G1 | G1 | 0 | Second cycle, 150 kBq/kg (2-mo interval) |
| | | | | | | | Third cycle, 125 kBq/kg (4-mo interval) |
| | | | | | | | OS 20 mo (death not tumor-related) |
| 10 | 13.4 | NA | NA | NA | G1 | 0 | Second cycle, 100 kBq/kg (2-mo interval) |
| | | | | | | | Third cycle, 100 kBq/kg (2-mo interval) |
| | | | | | | | Fourth cycle, 100 kBq/kg (2-mo interval) |
| | | | | | | | Combination with cabazitaxel 10 mg/m$^2$ → G3 thrombocytopenia, G3 neutropenia |
| | | | | | | | OS 12 mo |
| 11 | 14.3 | 0 | 0 | 0 | G2 | 0 | Second cycle, 100 kBq/kg (4-mo interval) |
| | | | | | | | Switched to TACE; OS 12 mo |
| 12 | 14.6 | 0 | 0 | 0 | G1 | 0 | Switched to TACE; OS 4 mo |
| 13 | 16.5 | G1 → G2 | G3 | G1 → G2 | G1 | 0 | Second cycle, 50 kBq/kg (2-mo interval) |
| | | | | | | | Third cycle, 50 kBq/kg (2-mo interval) |
| | | | | | | | OS 7 mo |
| 14 | 19.1 | 0 | 0 | 0 | G2 | Nausea G1, fatigue G2, xerophtalmia G2 | Discontinued (xerostomia/xerophtalmia) |
| | | | | | | | OS > 12 mo (lost to follow-up) |

PLT = platelets; WBC = white blood cells (total); Hb = hemoglobin; BSC = best supportive care; PFS = progression free survival; OS = overall survival, TD = transfusion dependent.



UH & EURATOM Exhibit 2044-003
Fusion v. Universität Heidelberg, et al.
IPR2023-00551

**TABLE 3**
Dosimetry of Dose-Limiting Organs with Different PSMA Ligands

| Dose-limiting organ | This work | | Zechmann et al. (*24*) | | Kratochwil et al. (*1*) | |
|---|---|---|---|---|---|---|
| | $^{225}$Ac-PSMA-617 ($Sv_{RBE5}$/MBq) | $^{225}$Ac-PSMA-617 ($Sv_{RBE5}$/7.4 MBq) | $^{131}$I-MIP-1095 (Gy/GBq) | $^{131}$I-MIP-1095 (Gy/3.7 GBq) | $^{177}$Lu-PSMA-617 (Gy/GBq) | $^{177}$Lu-PSMA-617 (Gy/7.4 GBq) |
| Salivary glands | 2.33 | 17.24 | 4.62 | 17.09 | 1.38 | 10.21 |
| Kidneys | 0.74 | 5.48 | 1.45 | 5.37 | 0.75 | 5.55 |
| Red marrow | 0.05 | 0.37 | 0.31 | 1.15 | 0.03 | 0.22 |

baseline. The follow-up exam was scheduled after 3 cycles in patients with biochemical response or already earlier in the case of clinical indication.

## RESULTS

### Patients

The selection of end-stage patients who had already exhausted approved options led to a heavily pretreated patient cohort. Seventy-one percent of the patients had previously received docetaxel, which is a larger fraction than the 56% patients considered suitable for chemotherapy in the ALSYMPCA trial (*22*). Secondary hormone manipulations (abiraterone, enzalutamide) and in the bone-confined patients $^{223}$Ra had also been used regularly. Patients were also included into regular clinical trials (cabozantinib, tasquinimod, sorafenib) with priority; some had history of less common second-line chemotherapeutics such as estramustine, cabazitaxel, or vinorelbine. The cohort is also unfavorable in regard to visceral metastasis, which is associated with poor prognosis (*23*), as well as extent of bone and bone marrow involvement (superscan pattern: $n = 6$) and reduced blood cell count at baseline. In this adverse setting, we observed a median overall survival of 8.5 mo (Table 2, last column).

### Dosimetry

For $^{225}$Ac-PSMA-617, salivary glands (2.3 $Sv_{RBE5}$/MBq), kidneys (0.7 $Sv_{RBE5}$/MBq), and red marrow (0.05 $Sv_{RBE5}$/MBq) are potentially dose-limiting organs. These values are similar to those reported for $^{131}$I-MIP-1095 (*24*) and $^{177}$Lu-PSMA-617 (*1*) as presented in Table 3 but for MBq instead of GBq activities. Other OLINDA results can be found in the Supplemental Table 1. All organ-absorbed doses consist of about 99.4% α- (considering RBE = 5), 0.5% β-, and 0.1% photon radiation, respectively.

### Microscopic PSMA Distribution Within Dose-Limiting Organs

A representative example of PSMA immunochemistry staining of salivary glands, kidneys, and prostate cancer is presented in (Fig. 1). In the salivary glands, staining of PSMA protein is found in focal hot spots of acinar cells preferably along their luminal border but not homogeneously dispersed within the parenchyma (Fig. 1A). In the kidneys, the PSMA protein is found in a selected subset of tubular cells again with a predominant luminal staining pattern (Fig. 1B). As a control, prostate cancer presents with intense PSMA staining (Fig. 1C).

### Empiric Dose Finding

No measurable changes in liver and kidney laboratory tests were observed. Acute hematologic and other side effects are summarized in Table 2. Two patients were excluded from hematologic toxicity analysis due to overlap with chemotherapy; 1 of them presented with grade 3 thrombocytopenia and neutropenia and 1 patient even died by neutropenic complications (grade 5). No treatment-related hematologic grade 3/4 and only 1 combined grade 2 thrombocytopenia/leucopenia occurred in the 200 kBq/kg group. Diffuse type red marrow infiltration was no predictor for increased hematologic toxicity as illustrated by the casuistic of a patient who had to discontinue $^{177}$Lu-PSMA-617 therapy due to hematologic toxicity but demonstrated remarkable response and tolerability to $^{223}$Ra and also tolerated $^{225}$Ac-PSMA-617 well after restratification due to PSMA-positive brain lesions (Fig. 2). Xerostomia was regularly reported with 100 kBq/kg or more per cycle and was considered intolerable with greater than 150 kBq/kg. Typically, first symptoms of xerostomia were observed 2–5 d after therapy injection, enduring for about 2 mo. If no succeeding cycle was indicated at this time there was a partial recovery, but some loss of secretion function appeared to be chronic. One patient in the 200 kBq/kg group reported dry eyes that had to be palliated by eye drops. This patient also reported fatigue and unspecific epigastric discomfort and was also the patient with the highest absolute treatment activity (patient 14). Despite

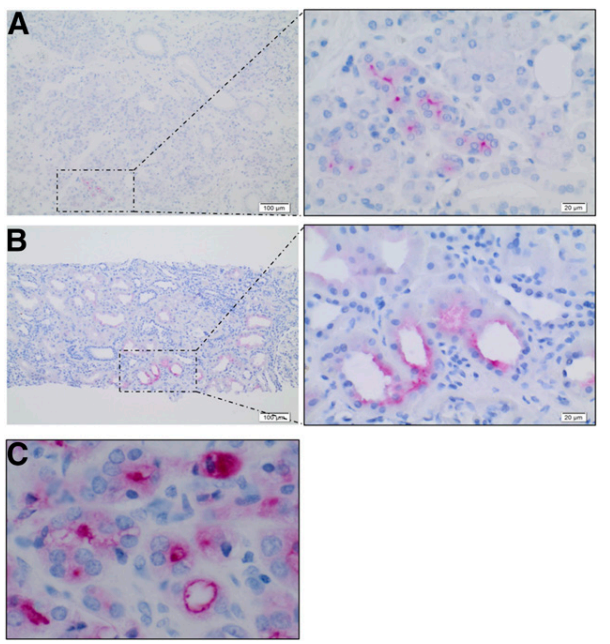


**FIGURE 1.** PSMA immunochemistry staining of salivary glands (A), kidney parenchyma (B), and prostate cancer (C).



**UH & EURATOM Exhibit 2044-004**
**Fusion v. Universität Heidelberg, et al.**
**IPR2023-00551**

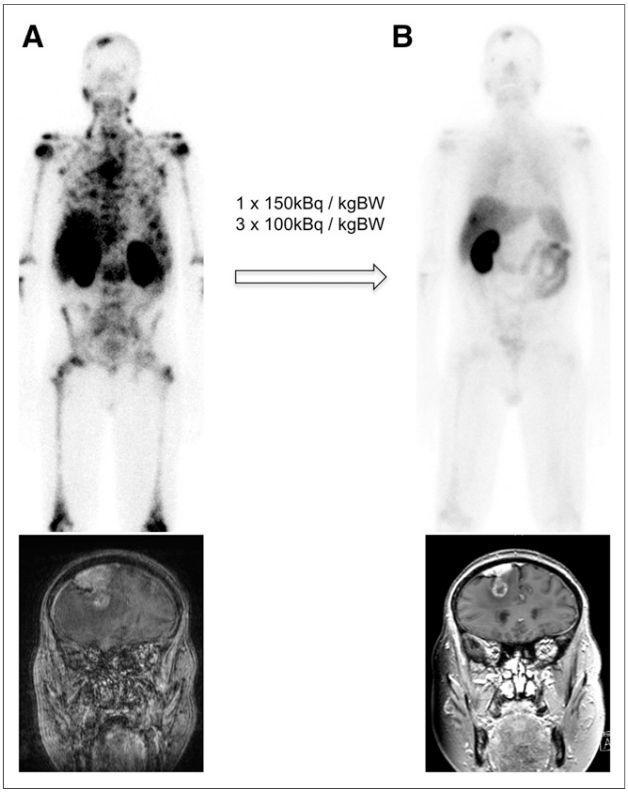


**FIGURE 2.** (A) At baseline, a patient presented with diffuse-type red marrow infiltration visualized with $^{99m}$Tc-MIP1427 PSMA scintigraphy (top) and brain metastasis (bottom). (B) Imaging follow-up 8 mo later presented partial response in bone (top) and brain (bottom).

promising antitumor activity, all patients in the 200 kBq/kg group and 1 of 2 patients in the 150 kBq/kg group discontinued therapy or insisted on dose reduction. Three patients initiated high caloric supplemental nutrition, because of weight loss, which was considered consecutively to the xerostomia by patient's self-reporting; however, no parenteral nutrition (grade 4 toxicity) had to be applied. Thus, we consider 100 kBq/kg of body weight (kgBW) the maximum tolerable dose, with xerostomia/xerophtalmia being the dose-limiting factor.

For 2 patients with PSA-negative tumor at baseline and the patients who overlappingly received other treatments, biochemical response assessment was not possible. The PSA-negative patients were reevaluated with PSMA PET/CT. One patient, treated with 50 kBq/kg activities, demonstrated progression, and the other patient, treated with 200 kBq/kg, showed a promising radiologic response (Fig. 3). For evaluable subjects, wk-8 PSA response demonstrated a tumor marker decline for all patients treated with more than 50 kBq/kg (Fig. 4).

With the limitation of small patient number, 100 kBq/kgBW was considered the treatment activity with the highest therapeutic range for this kind of patient (Fig. 5). However, because treatment activities were chosen depending on clinical risk factors, no reliable dose–response relationship can be derived.

### Effect of Repeated Dosing

Dose and timing of succeeding cycles are summarized in the last column of Table 2. In sum, 8 patients had further applications of $^{225}$Ac-PSMA-617. The therapeutic management was not defined prospectively but on individual decisions. One patient (patient 8) had favorable response after 2 cycles, and further applications were postponed until clinical demand ethically justified another application of experimental therapy. However, response to the second series, performed 1 y after first application, was short and the patient soon became resistant. A similar effect was observed in a patient who was treated in 4-mo intervals; after favorable biochemical response to the first cycle, succeeding cycles postponed until PSA relapse were remarkably less effective than the original course (individual course of PSA presented as Supplemental Fig. 2A). In contrast, applications every 2 mo in at least 100 kBq/kg doses resulted in a continuous decline of PSA (Supplemental Fig. 2B) over 2–4 cycles (patients 8, 9, and 10). Patients starting with or reducing to 50 kBq/kg became resistant after 1–2 cycles. No statistical analysis was reasonable with this low patient number and individualized treatment regimens.

## DISCUSSION

The aim of this work was to establish a treatment protocol for clinical application of $^{225}$Ac-PSMA-617 TAT in advanced-stage mCRPC, taking into account dosimetry considerations amended by empiric observations derived during first clinical experiences.

Recently a German multicenter study reported promising initial results for a subgroup of patients treated with $^{177}$Lu-PSMA-617 (*2*), but 40% of the patients presented with no PSA response at all. TAT with $^{213}$Bi-DOTATOC already demonstrated a potential to

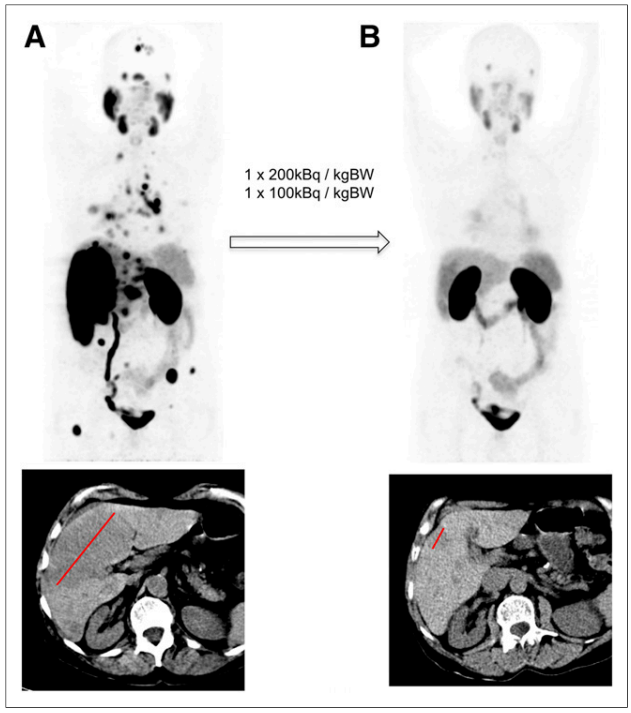


**FIGURE 3.** Baseline (A) and restaging (B) for a PSA-negative patient with histologically proven lung and liver metastases of prostate cancer was done with $^{68}$Ga-PSMA-11 PET (maximum-intensity projection, top) and CT (bottom), respectively. Promising antitumor activity in bone, liver, and pulmonal lesions have been observed, but also atrophy of salivary glands. Brain lesions were simultaneously treated with percutaneous radiotherapy.



UH & EURATOM Exhibit 2044-005
Fusion v. Universität Heidelberg, et al.
IPR2023-00551

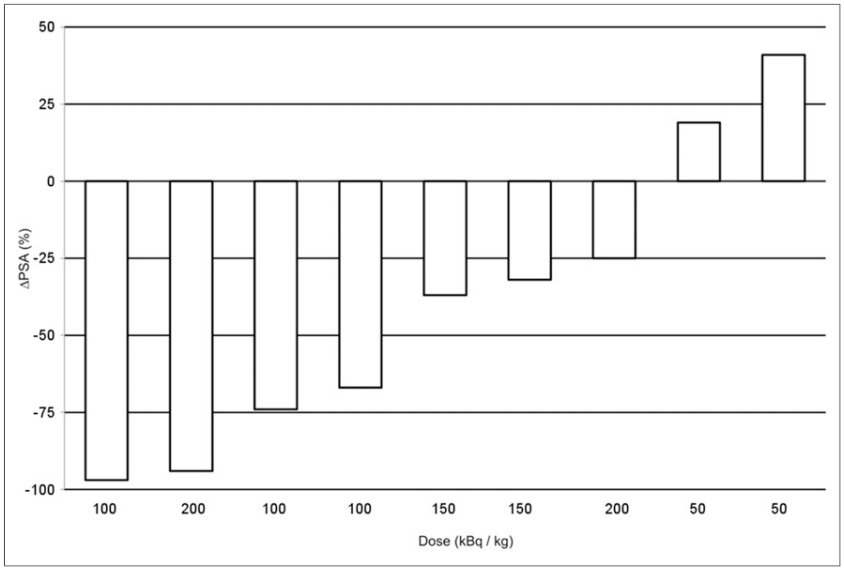


**FIGURE 4.** Waterfall graph of PSA response in evaluable patients. PSA response was observed in 75% of patients. No dose–response correlation was observed the 100–200 kBq/kgBW treatment activities.

break radio-resistance against $^{90}$Y-/$^{177}$Lu-DOTATOC (*4*), making it also highly reasonable that $^{225}$Ac-PSMA-617 will further improve the response rate in comparison to $^{177}$Lu-PSMA-617. The high rate of biochemical or radiologic responses in our cohort of heavily pretreated patients is already promising. Nevertheless, because of low patient number and variable treatment regimens it is not yet legitimate to start a discussion about efficacy in comparison to $^{177}$Lu-PSMA-617.

The radiobiologic specifics of TAT have already been reviewed in-depth (*14*). Specific background information relevant for understanding the characteristics of $^{225}$Ac are provided in the supplemental materials.

Preliminary considerations of safety dosimetry were done to define the appropriate dimension for starting activity before the first application of $^{225}$Ac-PSMA-617. For this reason, time–activity curves of representative $^{177}$Lu-PSMA-617 dosimetry scans were extrapolated to the half-life of $^{225}$Ac under the assumption that all daughter nuclides decay without relevant translocation. This can be assumed due to the rapid cellular internalization and storage of the carrier molecule PSMA-617 after binding to PSMA (*25*) and preclinical findings with an internalizing PSMA antibody that the intracytosolic-generated daughter nuclides predominantly remain inside the tumor (*26*). Although the simplification of instant decay may be widely true for $^{221}$Fr (half-life, 4.8 min) and $^{217}$At (half-life, 33 ms), a small percentage of $^{213}$Bi (half-life, 45.6 min) might leave the targeted cell by passive diffusion, introducing 1 source of uncertainty. Another critical point is that clinical imaging modalities are limited to millimeter resolution; thus, the nonuniform biodistribution of the radiopharmaceutical on the microscopic level cannot be evaluated in human beings and has to be discussed on the basis of preclinical data.

Assuming homogeneous distribution, we calculated a red marrow dose of 0.05 $Sv_{RBE5}$/MBq. For cell level microdosimetry, the radionuclide–to–cell nucleus geometry, that is, if the α-particle is emitted from extracellular or intracellular compartments, can be relevant. According to the pharmacokinetics of PSMA-617 (*1*), we consider passive diffusion into the extracellular body water fraction of the red marrow but no specific binding. Thus, the radiation geometry should be similar to an already preclinically evaluated α-radiopharmaceutical for which an RBE of only approximately 1 was suggested in regard to marrow toxicity (*27*) and the RBE of 5 used for the dosimetry estimate presented in Table 3 may be overcautious, which vice versa is well in line with the remarkably low hematologic toxicity observed in patients. Diffuse-type red marrow infiltration was considered a risk factor for increased hematologic toxicity during $^{177}$Lu-PSMA-617 therapy (*1*). Conventional dosimetry neglects the dose contribution of bone metastases to the red marrow because it cannot easily be modeled. However, in the case of red marrow carcinosis this effect may be of particular impact with the mean/maximum of 0.5/2 mm (20/80 cell diameters) tissue range of $^{177}$Lu β-particles. In contrast, the 47- to 85-μm (2–3 cell diameters) tissue ranges of $^{225}$Ac α-particles (Supplemental Fig. 3) theoretically offer selective tumor cell kill. Both effects provide an explanation that a patient with suggestive red marrow infiltration (Fig. 2) and history of myelosuppression after 4 GBq of $^{177}$Lu-PSMA-617 (0.12 Gy taking into account only perfusion-dependent effects) could still tolerate 13.4 MBq of $^{225}$Ac-PSMA-617 (0.67 $Sv_{RBE5}$); this case exquisitely illustrates the methodical limitations of dosimetry and warns about an uncritical reliance on dosimetry estimates of dose-limiting organs (Table 3). We also want to point out our unpleasant experience with 2 patients (G3 and G5 toxicity) in whom chemotherapy was initiated with less than an 8-wk interval after TAT (assumed prudent by their oncologists due to nonmeasurable hematologic toxicity)

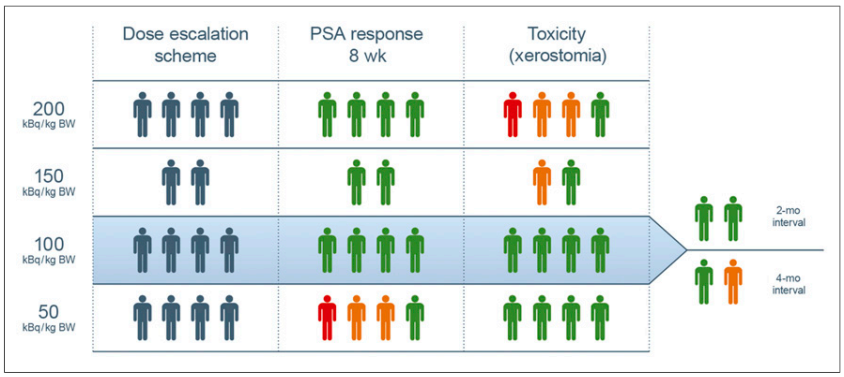


**FIGURE 5.** Reasonable treatment corridor between insufficient treatment response (red: patient died before reevaluation; orange: PSA progression; green: imaging or PSA response) and intolerable toxicity (red: xerophthalmia; orange: xerostomia G2; green: no or only G1 xerostomia). During repeated therapies, insufficient PSA response was observed at 4-mo interval.



UH & EURATOM Exhibit 2044-006
Fusion v. Universität Heidelberg, et al.
IPR2023-00551

because low hematologic toxicity might also tempt other physicians/researchers into combination therapies, but they should be prepared for the possibility of overadditive toxicity.

Average kidney-absorbed dose was calculated with 0.7 $Sv_{RBE5}$/MBq. Suborgan distribution acquired with an α-camera and microscale dosimetry modeling have already been published for a $^{211}$At-labeled urea-based PSMA ligand in the kidneys of mice (*7*). The authors reported dose-limiting nephropathy as validated with histopathology and laboratory tests. In their suborgan dosimetry, hot spots in the proximal tubules were 3-fold higher than in glomeruli (123 vs. 42 Gy/MBq) and 5-fold higher than average organ dose, illustrating the limitations of imaging-based dosimetry in regards to TAT. The mean kidney-absorbed dose for the $^{211}$At-PSMA TAT in mice was 24.6 Gy/MBq (123 $Sv_{RBE5}$/MBq in our nomenclature), 0.037 MBq were nontoxic, and the treatment dose lethal to 10% of the exposed kidneys was 0.111 MBq, which would correspond to 4.6–13.7 $Sv_{RBE5}$. Mild proteinuria developed after therapy, but resolved over time; therefore, this maximum-tolerated dose of mice only reflects a single treatment cycle but not the maximum cumulative dose. In our patient collective, we did not exceed this dose range and no acute or subacute renal toxicity was observed. However, kidneys are well-known late reacting organs to radiation therapy and onset of radiation-induced renal dysfunction can appear years later and might be missed with our short follow-up period. Therefore, we cannot rule out that cumulative kidney dose is the limiting factor for PSMA TAT, requiring thoroughly long-term follow-up of renal function, especially once PSMA TAT might be used in earlier tumor stages.

Immunostainings of salivary glands (Fig. 1A) reveal rather spot-type than disseminated distribution of PSMA-positive cells, and wide parts of gland parenchyma are spatially well separated from these hot spots, with distances easily exceeding the penetration depth of the α-particle. If uptake of $^{225}$Ac-PSMA-617 would be only PSMA-specific, we would expect less toxicity for salivary glands than with β-emitters. However, this was opposed by clinical findings when severe xerostomia and in 1 case dry eyes became the dose-limiting factor for $^{225}$Ac-PSMA-617, exceeding the clinical toxicities of $^{131}$I-MIP1095 at comparable effective absorbed dose (Table 3). Probably the high uptake in salivary glands is not PSMA-dependent but might be caused by small-molecule transporters. This thesis is supported by an imaging study of radiolabeled PSMA antibodies that present much lower uptake in salivary glands (*28*). Moreover, the long retention time of PSMA-617 in glands implies internalization, and for disintegrations closely related to the nucleus, an RBE of 5 might present an underestimation. Unfortunately, xerostomia was partially irreversible. Chronic G1 toxicity (coping water) is typically tolerated by most patients but already the need for saliva-substitution sprays and gels is rated a remarkable loss of quality of life by some patients.

Because the preliminary dosimetry modeling contains relevant uncertainties, an empiric dose escalation was necessary to exploit the ideal therapeutic range of $^{225}$Ac-PSMA-617. Empiric dose finding is the typical approach for conventional chemotherapy and was also applied in early phase $^{223}$Ra trials (*29*) when safety was evaluated using adverse events, which then were used to define the maximum-tolerated dose. Similar to all early phase dose finding studies, 1 limitation of this report is low patient number and eventually some adverse events might have been observed or missed rather by chance than after robust statistics. However, the good tolerability also of $^{225}$Ac-PSMA-617 is well in line with the few adverse events observed under $^{177}$Lu-PSMA-617 (*30*). It is important to note that the patients receiving 50 kBq/kgBW were the most challenging ones from the very start and the low treatment activity was chosen by the responsive physician, for example, due to grade 4 myelosuppression at baseline. On the other hand, the highest treatment activity was offered only to patients with brain or liver metastases, who present the most adverse prognostic factors. Therefore, it is reasonable that in regard to PSA response no dose–response relationship was observed. Thus, it is premature to conclude that the 50 kBq/kgBW dose is completely ineffective. However, the patient collective currently qualified for experimental therapy presents with high tumor burden and aggressive metastasis. Consequently, early onset of positive treatment effects is necessary to ameliorate these challenging patients at all. Once $^{225}$Ac-PSMA-617 is investigated for treatment of earlier tumor stages, the efficacy of low-dose regimens should be reevaluated in respect to reduction of side effects.

On the basis of our preliminary data, a treatment activity of 100 kBq/kg administered every 2 mo was found to provide promising response with tolerable side effects (Fig. 4). Evaluation of response rate and duration of tumor control is out of the scope of this study. Nevertheless, when the unfavorable prognostic profile of the patient cohort is taken into account, the observed antitumor activity of $^{225}$Ac-PSMA-617 is more than promising.

## CONCLUSION

On the basis of our initial clinical experience with advanced patients, a treatment activity of 100 kBq/kg of $^{225}$Ac-PSMA-617 is tolerable and presents promising antitumor activity. Repeated treatments in intervals of 8 wk may lead to continuing tumor control. This protocol is now routinely applied for salvage therapy of end-stage mCRPC patients in our clinic. Formal clinical trials in larger patient cohorts are warranted to further investigate the potential of $^{225}$Ac-PSMA-617 TAT in a prospective manner.

## DISCLOSURE

A patent application for PSMA-617 (regardless of the radiolabeling nuclide) is held by Uwe Haberkorn. No other potential conflict of interest relevant to this article was reported.


## ACKNOWLEDGMENTS

We thank the Tissue Bank of the National Center of Tumor Diseases (NCT) for the supply of tissue samples from salivary glands, kidneys, and prostate cancer. We thank Mike Reiss for graphical support.


## REFERENCES


1. Kratochwil C, Giesel FL, Stefanova M, et al. PSMA-targeted radionuclide therapy of metastatic castration-resistant prostate cancer with $^{177}$Lu-labeled PSMA-617. *J Nucl Med.* 2016;57:1170–1176.
2. Rahbar K, Ahmadzadehfar H, Kratochwil C, et al. German multicenter study investigating $^{177}$Lu-PSMA-617 radioligand therapy in advanced prostate cancer patients. *J Nucl Med.* 2017;58:85–90.
3. Heck MM, Retz M, D'Alessandria C, et al. Systemic radioligand therapy with $^{177}$Lu labeled prostate specific membrane antigen ligand for imaging and therapy in patients with metastatic castration resistant prostate cancer. *J Urol.* 2016;196:382–391.
4. Kratochwil C, Giesel FL, Bruchertseifer F, et al. $^{213}$Bi-DOTATOC receptor-targeted alpha-radionuclide therapy induces remission in neuroendocrine tumours refractory to beta radiation: a first-in-human experience. *Eur J Nucl Med Mol Imaging.* 2014;41:2106–2119.
5. Liu H, Rajasekaran AK, Moy P, et al. Constitutive and antibody-induced internalization of prostate-specific membrane antigen. *Cancer Res.* 1998;58:4055–4060.





**UH & EURATOM Exhibit 2044-007**
**Fusion v. Universität Heidelberg, et al.**
**IPR2023-00551**

6. Kiess AP, Minn I, Chen Y, et al. Auger radiopharmaceutical therapy targeting prostate-specific membrane antigen. *J Nucl Med.* 2015;56:1401–1407.
7. Kiess AP, Minn I, Vaidyanathan G, et al. (2S)-2-(3-(1-carboxy-5-(4-$^{211}$At-astatobenzamido)pentyl)ureido)-pentanedioic acid for PSMA-targeted α-particle radiopharmaceutical therapy. *J Nucl Med.* 2016;57:1569–1575.
8. Rubini G, Nicoletti A, Rubini D, Asabella AN. Radiometabolic treatment of bone-metastasizing cancer: from 186rhenium to 223radium. *Cancer Biother Radiopharm.* 2014;29:1–11.
9. Kabasakal L, AbuQbeitah M, Aygün A, et al. Pre-therapeutic dosimetry of normal organs and tissues of $^{177}$Lu-PSMA-617 prostate-specific membrane antigen (PSMA) inhibitor in patients with castration-resistant prostate cancer. *Eur J Nucl Med Mol Imaging.* 2015;42:1976–1983.
10. Delker A, Fendler WP, Kratochwil C, et al. Dosimetry for $^{177}$Lu-DKFZ-PSMA-617: a new radiopharmaceutical for the treatment of metastatic prostate cancer. *Eur J Nucl Med Mol Imaging.* 2016;43:42–51.
11. Yadav MP, Ballal S, Tripathi M, et al. Post-therapeutic dosimetry of $^{177}$Lu-DKFZ-PSMA-617 in the treatment of patients with metastatic castration-resistant prostate cancer. *Nucl Med Commun.* 2017;38:91–98.
12. Silver DA, Pellicer I, Fair WR, Heston WD, Cordon-Cardo C. Prostatespecific membrane antigen expression in normal and malignant human tissues. *Clin Cancer Res.* 1997;3:81–85.
13. Stabin MG, Sparks RB, Crowe E. OLINDA/EXM: the second-generation personal computer software for internal dose assessment in nuclear medicine. *J Nucl Med.* 2005;46:1023–1027.
14. Sgouros G, Roeske JC, McDevitt MR, et al. MIRD pamphlet no. 22 (abridged): radiobiology and dosimetry of α-particle emitters for targeted radionuclide therapy. *J Nucl Med.* 2010;51:311–328.
15. Giesel FL, Hadaschik B, Cardinale J, et al. F-18 labelled PSMA-1007: biodistribution, radiation dosimetry and histopathological validation of tumor lesions in prostate cancer patients. *Eur J Nucl Med Mol Imaging.* 2017;44:678–688.
16. Lu G, Maresca KP, Hillier SM, et al. Synthesis and SAR of $^{99}$mTc/Re-labeled small molecule prostate specific membrane antigen inhibitors with novel polar chelates. *Bioorg Med Chem Lett.* 2013;23:1557–1563.
17. Apostolidis C, Molinet R, Rasmussen G, Morgenstern A. Production of Ac-225 from Th-229 for targeted alpha therapy. *Anal Chem.* 2005;77:6288–6291.
18. Zielinska B, Apostolidis C, Bruchertseifer F, Morgenstern A. An improved method for the production of Ac-225/Bi-213 from Th-229 for targeted alpha therapy. *Solvent Extr Ion Exch.* 2007;25:339–349.
19. Eder M, Neels O, Müller M, et al. Novel preclinical and radiopharmaceutical aspects of [$^{68}$Ga]Ga-PSMA-HBED-CC: a new PET tracer for imaging of prostate cancer. *Pharmaceuticals (Basel).* 2014;7:779–796.
20. Kratochwil C, Bruchertseifer F, Giesel FL, et al. $^{225}$Ac-PSMA-617 for PSMA-targeted α-radiation therapy of metastatic castration-resistant prostate cancer. *J Nucl Med.* 2016;57:1941–1944.
21. Common Terminology Criteria for Adverse Events (CTCAE), version 4.03 (NIH/NCI). National Cancer Institute website. http://evs.nci.nih.gov/ftp1/CTCAE/CTCAE_4.03_2010-06-14_QuickReference_8.5x11.pdf. Accessed June 30, 2017.
22. Parker C, Nilsson S, Heinrich D, et al. Alpha emitter radium-223 and survival in metastatic prostate cancer. *N Engl J Med.* 2013;369:213–223.
23. Pond GR, Sonpavde G, de Wit R, Eisenberger MA, Tannock IF, Armstrong AJ. The prognostic importance of metastatic site in men with metastatic castration-resistant prostate cancer. *Eur Urol.* 2014;65:3–6.
24. Zechmann CM, Afshar-Oromieh A, Armor T, et al. Radiation dosimetry and first therapy results with a (124)I/(131)I-labeled small molecule (MIP-1095) targeting PSMA for prostate cancer therapy. *Eur J Nucl Med Mol Imaging.* 2014;41:1280–1292.
25. Benešová M, Schäfer M, Bauder-Wüst U, et al. Preclinical evaluation of a tailor-made DOTA-conjugated PSMA inhibitor with optimized linker moiety for imaging and endoradiotherapy of prostate cancer. *J Nucl Med.* 2015;56:914–920.
26. McDevitt MR, Ma D, Lai LT, et al. Tumor therapy with targeted atomic nanogenerators. *Science.* 2001;294:1537–1540.
27. Behr TM, Behe M, Stabin MG, et al. High-linear energy transfer (LET) alpha versus low-LET beta emitters in radioimmunotherapy of solid tumors: therapeutic efficacy and dose-limiting toxicity of $^{213}$Bi- versus $^{90}$Y-labeled CO17-1A Fab' fragments in a human colonic cancer model. *Cancer Res.* 1999;59:2635–2643.
28. Pandit-Taskar N, O'Donoghue JA, Ruan S, et al. First-in-human imaging with $^{89}$Zr-Df-IAB2M anti-PSMA minibody in patients with metastatic prostate cancer: pharmacokinetics, biodistribution, dosimetry, and lesion uptake. *J Nucl Med.* 2016;57:1858–1864.
29. Carrasquillo JA, O'Donoghue JA, Pandit-Taskar N, et al. Phase I pharmacokinetic and biodistribution study with escalating doses of $^{223}$Ra-dichloride in men with castration-resistant metastatic prostate cancer. *Eur J Nucl Med Mol Imaging.* 2013;40:1384–1393.
30. Yadav MP, Ballal S, Tripathi M, et al. $^{177}$Lu-DKFZ-PSMA-617 therapy in metastatic castration resistant prostate cancer: safety, efficacy, and quality of life assessment. *Eur J Nucl Med Mol Imaging.* 2017;44:81–91.



**UH & EURATOM Exhibit 2044-008**
**Fusion v. Universität Heidelberg, et al.**
**IPR2023-00551**